ROYAL SOCIETY OF CHEMISTRY

Soft Matter

PAPER

The energy of fcc and hcp foams†

S. Hutzler, *[a] F. F. Dunne,[a] A. M. Kraynik[ab] and D. Weaire[a]

Cite this: DOI: 10.1039/d0sm00820f

We present Surface Evolver evaluations of the difference in energy between face-centred cubic (fcc) and hexagonal close-packed (hcp) foams in the usual idealized model, for liquid fractions ranging from the dry to the wet limit. The difference vanishes in both limits, and favours hcp for all intermediate liquid fractions, as has been proven. The maximum relative energy difference is very small, of the order of 10^{-5}. The asymptotic dependence on liquid fraction is non-analytic in both limits: we present explicit expressions in both cases, derived from first principles. They have been obtained from identifying node interactions (dry limit) and contact interactions (wet limit) as the respective sources for energy differences between fcc and hcp. The wet limit is well described by Morse–Witten theory which has proven to be very powerful for the analytic computation of the surface energy of slightly deformed bubbles.

Received 7th May 2020,
Accepted 1st August 2020

DOI: 10.1039/d0sm00820f

rsc.li/soft-matter-journal

1 Introduction

The comparison of the energies of face-centred cubic (fcc) and hexagonal close-packed (hcp) foams has turned out to be a stimulating testing ground for ideas and methods that are central to the wider field of foam structures in general.[1–3] In the present paper we push numerical simulations to a very high level of accuracy in order to accurately determine such relative energies. We offer interpretations of the most salient results, which relate to the approach to the wet and dry limits, respectively, at liquid fractions $\phi_c = 1 - \pi/(3\sqrt{2}) \simeq 0.26$ and zero. In the wet limit this is achieved *via* an exploration of the Morse–Witten theory for bubble interaction. For the dry limit we have developed a non-analytic term accounting for node interaction which is to be added to the established expansion of energy in terms of liquid fraction.

The questions raised and answered for these ordered monodisperse close-packed structures might be considered esoteric, since foams are typically disordered and polydisperse. However, monodisperse foams of sufficiently high liquid fraction have been found to crystallise in close-packed structures. Originally discovered by Bragg and Nye in 1947,[4] and subsequently ignored, this has been a subject of renewed investigation in more recent times.[5–11] Despite this, the topic remains largely unexplored; the present work is relevant to its future development.

In the usual idealized model of a foam,[1] illustrated in Fig. 1, infinitesimally thin films meet threefold, with contact angle zero, at finite size Plateau borders, which contain all the liquid.

In equilibrium, a foam has minimum surface energy; the contribution of an element of a film surface is twice that of an element of a Plateau border. The local geometrical/topological rules for stable equilibrium were identified a century and a half

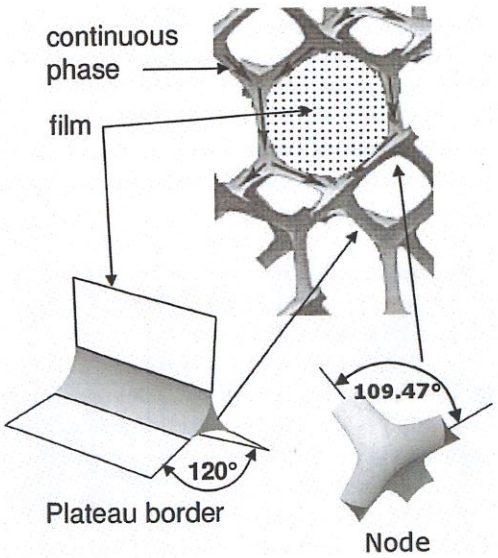

Fig. 1 Elements of foam structure in the case of low liquid volume fraction, $\phi \lesssim 0.05$. Three films meet at 120 degrees in Plateau borders, which in turn meet under angles of arcos (−1/3) ≃ 109.67° in a node or junction. In the idealised model all liquid is contained in the Plateau border network, *i.e.* the films are infinitesimally thin. (These angles are for $\phi = 0$.).

[a] School of Physics, Trinity College Dublin, The University of Dublin, Ireland. E-mail: stefan.hutzler@tcd.ie
[b] Retired from Sandia National Laboratories, Albuquerque, USA

† Electronic supplementary information (ESI) available. See DOI: 10.1039/d0sm00820f

ago,[12] and their implications for extended structures have been debated ever since.

The calculation of the precise energies of 2d foam structures had to wait until the 1980s[13,14] (but a good description of the fourfold junctions in 3d foams was given in a different context by Nye and Frank in 1973[15]).

The workhorse of this subject has been Brakke's Surface Evolver,[16] which has been steadily refined, so that systems of over a thousand bubbles can now be analysed with great accuracy.[17] In the present paper we begin by applying the Evolver to a particularly demanding special case, the small difference of the energies of the fcc and hcp structures. We then develop asymptotic formulae for this difference, applicable in the vicinity of the dry and wet limits; these are consistent with the numerical results over quite wide ranges.

Our analysis (which is equally applicable to ordered emulsions) breaks new ground in various respects, in order to isolate the higher-order contributions to energy which are responsible for the energy difference in question. It should stimulate further close attention to theory, but the present application is a very specialised one and generalisation will be difficult.

2 Hcp and fcc foams

The hcp and fcc structures (Fig. 2) are familiar from crystallography. Each consists of a stacking of close-packed 2d layers (ABAB and ABC in a familiar notation). In the case of hcp, we shall only consider the case of ideal axial ratio c/a for which all nearest neighbour distances are equal. This is not required by symmetry, and will be commented upon later. If bubbles of equal volume are centred at each point of Fig. 2, a foam is created in which the centre of mass of each bubble coincides with the corresponding point and thin films are formed at bubble-bubble contacts. Fig. 3 shows examples of hcp and fcc foams for several values of liquid fraction ϕ, generated using the Surface Evolver.

At $\phi = 0$ (dry foam) both fcc and hcp structures are unstable, as they do not conform to Plateau's rule, which requires there

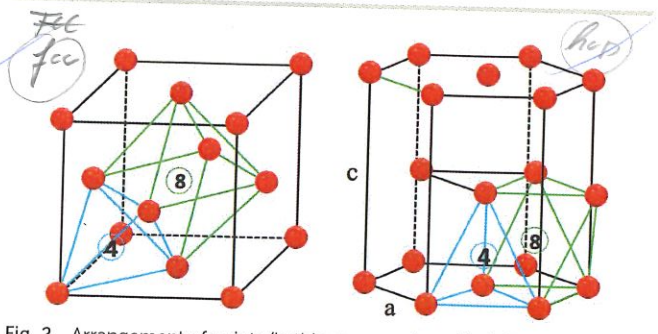

Fig. 2 Arrangement of points (in this case, centres of bubbles) in the face-centred cubic (fcc) and hexagonal close packed structures (hcp). The diagonal in this representation of the fcc lattice is the vertical axis in the hcp structure. We have also indicated the positions of a fourfold and an eightfold junction (node) of Plateau borders, placed respectively in the centre of a tetrahedron or octahedron. (See the discussion in Section 5.2.).

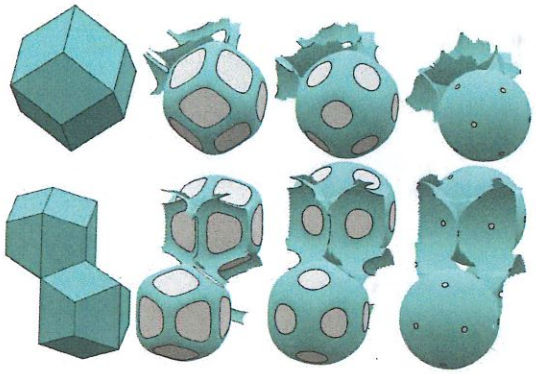

Fig. 3 Examples of bubbles generated using the Surface Evolver for monodisperse foams, arranged in (top) fcc and (bottom) hcp structures. They are shown (left to right) at the dry limit, $\phi = 0$ (where the bubbles are rhombic (fcc) or trapezo-rhombic (hcp) dodecahedra, although with some slightly curved interfaces), at $\phi = 0.04$, at $\phi = 0.11$ and at $\phi = 0.25$, close to the wet limit.

to be only four-fold vertices for stability. However, in Surface Evolver computer simulations the eight-fold vertices which occur in both fcc and hcp foams have been found to be stable for values of ϕ as low as 0.000278[18] (a result which disproved the earlier conjecture that a symmetric eight-fold vertex would be stable for any finite value of liquid fraction[19]). We shall ignore this instability in the present work. A higher, but still very small value of about 0.003 was found in microgravity experiments.[20]

Examples of monodisperse dry foams which adhere to Plateau's rules at $\phi = 0$ are the Kelvin structure[21,22] and the Weaire–Phelan structure.[23,24]

3 The wet and dry limits

Fig. 3 shows Surface Evolver generated images of bubbles arranged respectively in fcc and hcp, for four different values of liquid fraction.

In the wet limit, the bubbles take the form of perfect spheres (radius R) in contact, so that the energy per bubble is

$$E_0 = 4\pi\gamma R^2, \qquad (1)$$

where γ is surface tension. In this case the energies of both fcc and hcp are obviously equal. In the dry limit this is also self-evident, that is, the total areas of the plane faces of the polyhedral bubbles is the same for fcc and hcp, see Fig. 4. But how do the energies $E(\phi)$ compare for a general value of liquid fraction ϕ?

Whyte *et al.*[25] gave a rigorous proof that the fcc structure cannot have a lower energy than hcp for any liquid fraction, using a variational argument. Having established this, the question remains: what is the magnitude of the energy difference, favouring the hcp structure?

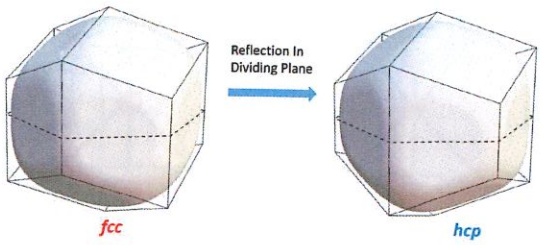

Fig. 4 In the dry limit ($\phi = 0$) a bubble in an fcc foam takes the form of a rhombic dodecahedron (solid lines, left). Reflection of its top half in the indicated dividing plane results in the trapezo-rhombic dodecahedron of a bubble in a hcp foam (solid lines, right) with the same total surface area (energy). For a finite value of ϕ the same operation transforms an fcc bubble (shaded bubble, left, here for $\phi \simeq 0.125$) into a trial solution for an hcp bubble (shaded bubble, right). Its surface area can be relaxed (for fixed bubble volume), resulting in a hcp bubble of lower energy than the fcc bubble; for details see ref. 25.

4 Computed energy difference for all liquid fractions

The Surface Evolver was used to calculate the energy of fcc and hcp foams for liquid fractions $0.01 \leq \phi \leq 0.25$ and bubble volume set to unity. The Surface Evolver input files were generated by taking the dry structures shown in Fig. 3 and applying the command, wetfoam2.cmd, to replace cell edges with primitive Plateau borders, *i.e.* the liquid-filled channels with triangular cross sections and flat faces, to be subsequently relaxed. High accuracy was achieved by refining the triangular mesh six times, taking a large number of iteration steps at each level of refinement, and using quadratic facets for the last three levels. This procedure typically produces foam energies with absolute accuracies of about six decimal places.

The fcc structure has cubic symmetry, which guarantees isotropic stress and minimum energy; however, the hcp structure only has hexagonal symmetry which does not guarantee isotropic stress (that is, in equilibrium the axial ratio does not have to take its ideal value). The magnitude of stress anisotropy was evaluated by calculating the stress of the hcp foam for $\phi = 0.11$, where the energy difference between hcp and fcc is greatest. The stress became isotropic when the distance between bubble layers was decreased about 0.03% (for $\phi = 0.11$); however, this resulted in an energy decrease only in the seventh decimal place. Consequently the stress anisotropy of the hcp foam structure is relatively insignificant and the ideal axial ratio is imposed in all of these calculations, and what follows. Of course, according to the variational principle, the energy difference can only increase if this restriction is relaxed.

Fig. 5 presents results for the energy difference between fcc and hcp over the full range of liquid fraction, ϕ, in the form of the dimensionless quantity $(E_{\mathrm{fcc}}(\phi) - E_{\mathrm{hcp}}(\phi))/E_0$. This energy difference is a very small quantity (with a maximum of about 9×10^{-6} for $\phi \simeq 0.11$), compared with the total energy of either structure (which has a maximum value of $E(\phi = 0)/E_0 \simeq 1.1$).

A close examination of Fig. 5 will detect an approach to zero energy difference which flattens out markedly in both wet and dry limits. This appears inconsistent with any simple power-law dependence.

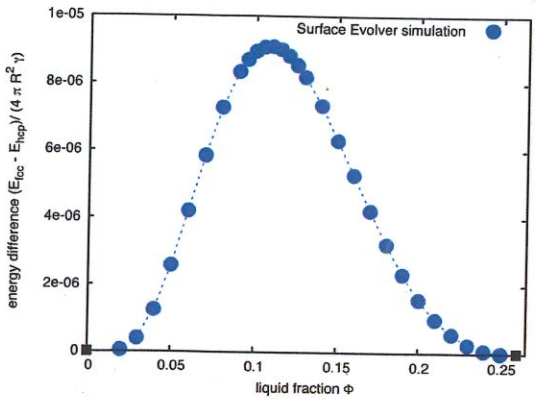

Fig. 5 Energy difference between fcc and hcp foams as a function of liquid fraction ϕ. The blue data points are computed using the Surface Evolver Software. The black squares mark the dry and wet limits, when the difference is zero. Note that close to both limits the energy difference flattens out markedly. In the wet limit bubbles have radius R and energy $4\pi R^2\gamma$: note the normalization.

5 Approach to the wet and dry limits

In order to shed some light on all of this we have concentrated on analyzing the limiting form in the vicinity of the wet and dry limits. In both cases asymptotic expressions for the difference will be developed. They are quite different but are both non-analytic, as the data suggests.

5.1 Wet limit

Close to the wet limit, contacting bubbles are deformed, modifying their spherical shapes, with the formation of thin films at the contact points; in fcc and hcp every bubble has 12 contacts.

Any theory that treats the contributions of each contact independently with a simple pairwise potential between representative points, dependent on their separation (as some *ad hoc* heuristic models have done in the modelling of foam properties) would yield *zero* for the hcp-fcc energy difference. We shall see that the relative *orientation* of contacting neighbours in the two cases is the source of the difference, in the wet regime. This dependence is far from obvious, and only comes to light when we adduce the theoretical method of Morse and Witten.[26] It was developed specifically for foams (or emulsions) close to the wet limit. Until recently, this remarkable development has not been well appreciated or understood and it has hardly been applied at all. Höhler and Weaire[27] have provided an exhaustive interpretation and explanation of the method and its justification, which may stimulate its wider use.

The first experimental confirmation of Morse–Witten theory appears to be that by Ginot *et al.*[28] who measured bubble deformation in a linear train of bubbles under gravity. The experimental data could not be explained using a model of pairwise interactions, but is well described within the framework of Morse–Witten theory. It is also supported by Surface Evolver simulations.

The present problem provides a very appropriate context in which to demonstrate the application of the theory, and the simplicity of some of its implications, for three dimensional foam structures.

Results derived from the theory are exact in an asymptotic sense: that is, they give forms for force, energy, *etc.* that are the leading terms as ϕ approaches the wet limit.

Remarkably, the theory shows that bubbles may be represented by points placed at their centres of mass, with central forces acting between them.[30] Crucially, each of these forces depends on the local arrangement and magnitudes of compressions of all of the contacts of the two interacting bubbles, not just the separation of their representative points. In that sense, the theory is "non-local". Because hcp and fcc have different arrangements of nearest neighbours, this dependence entails a finite energy difference and may be applied to the problem at hand.

Although challenging in some respects, including the appearance of logarithmic terms in the pairwise interactions, the application of the Morse–Witten theory to the present problem yields remarkably simple results, particularly a non-analytic exact asymptotic form for the energy difference in the vicinity of the wet limit.

In the Morse–Witten formulation the radial displacement x_i of the surface of a bubble at a given contact i is related to the magnitudes and directions of all of the forces, acting at contacts j of the bubble. Here displacement is a negative quantity, defined as the difference between the distance of the centre of mass to the contact point and the undeformed bubble radius, R. For a bubble of radius $R = 1$ and forces f_j normalized by γR, it is given by[27,30]

$$x_i = \frac{1}{24\pi}\left[5 + 6\ln\left(\frac{f_i}{8\pi}\right)\right]f_i - \sum_{j\neq i} G(\theta_{ij})f_j. \qquad (2)$$

Note the logarithmic term, a distinctive feature of the theory.[27] The sum is the contribution of the "non-local" forces f_j acting at all of the other contacts $j \neq i$. $G(\theta_{ij})$ is the Green's function,

$$G(\theta) = -\frac{1}{4\pi}\left[\frac{1}{2} + \frac{4}{3}\cos\theta + \cos\theta\ln\left(\sin^2\frac{\theta}{2}\right)\right], \qquad (3)$$

to be evaluated at the angles θ_{ij} between vectors pointing from the bubble centre to the contacts i and j. (See Fig. 6 for an illustration for hcp and fcc.)

The energy of a foam as a function of liquid fraction is often expressed as normalized excess energy $\varepsilon(\phi)$ per bubble, defined as,

$$\varepsilon(\phi) = E(\phi)/E_0 - 1, \qquad (4)$$

where E_0 is given by eqn (1).[3,29] In the Morse–Witten model this quantity, expressed in terms of the forces f_i acting at the N contacts of a bubble, is given by[26,27]

$$\varepsilon = \frac{1}{4\pi}\left(\frac{1}{8\pi}\sum_i^N f_i^2\left(\ln\frac{8\pi}{f_i} - \frac{4}{3}\right) + \frac{1}{2}\sum_{i,j\neq i}^N G(\theta_{ij})f_i f_j\right). \qquad (5)$$

For any given crystalline structure, such as fcc or hcp, the angles θ_{ij} between contacts are known and thus $G(\theta_{ij})$ is readily evaluated.

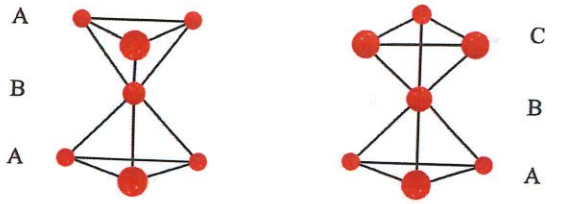

Fig. 6 Sketch showing the nearest neighbours of the central point for hcp and fcc. The energy difference between the two structures is due to the difference in angles θ_{ij} between neighbours above and below the horizontal plane containing the central point.

We will in the following show how eqns (2) and (5) can be employed to compute $\varepsilon(\phi)$ as a function of liquid fraction for both fcc and hcp, using the Morse–Witten model for displacements x_i that are the same for all contacts ($x_i = x$).

The displacement x and liquid fraction ϕ are related by

$$\frac{1-\phi}{1-\phi_c} = \frac{1}{(1+x)^3} \qquad (6)$$

for bubbles of spherical radius unity. The left hand side is the ratio of gas fraction to its critical value; gas volume is constant and total volume scales inversely with $(1 + x)^3$.

5.1.1 Energy of fcc structure. As a preliminary exercise, we shall explore the energy of the fcc structure, as given by Morse–Witten theory.

All forces f_i acting on a given bubble, are equal by symmetry, as are the displacements x_i. The theory gives energy as a function of f, eqn (5), but we wish to know it as a function of x (hence ϕ).

From eqn (2), and evaluating $G(\theta)$, eqn (3), at the 11 angles θ_{ij} for fcc ($\frac{\pi}{3}$ (4 times), $\frac{2\pi}{3}$ (4 times), $\frac{\pi}{2}$ (twice), π (once)) we obtain the displacement $x(f)$ at each contact,

$$x(f) = \frac{f}{4\pi}\left(\ln\frac{f}{8\pi} + 5 - 2\ln 3\right). \qquad (7)$$

This may be formally inverted by using the lower branch of the Lambert W function (resulting in $f(x) = 4\pi x/W_{-1}(e^5 x/18)$);[27] however, this will be avoided in what follows.

For force $f \ll 1$ the following asymptotic form can be obtained from eqn (7)[27]

$$f \sim \frac{4\pi x}{\ln(-x)}. \qquad (8)$$

An expression for normalized excess energy as a function of force is then obtained from eqn (5),

$$\varepsilon_{fcc}(f) = \frac{3}{8\pi^2}f^2(-\ln f - 11/2 + \ln 8 + \ln 9 + \ln\pi). \qquad (9)$$

Inserting the asymptotic expression ($f \ll 1$) for $f(x)$ (eqn (8)) results in

$$\varepsilon_{fcc}(\phi) \sim -6\frac{x^2(\phi)}{\ln[-x(\phi)]}, \qquad (10)$$

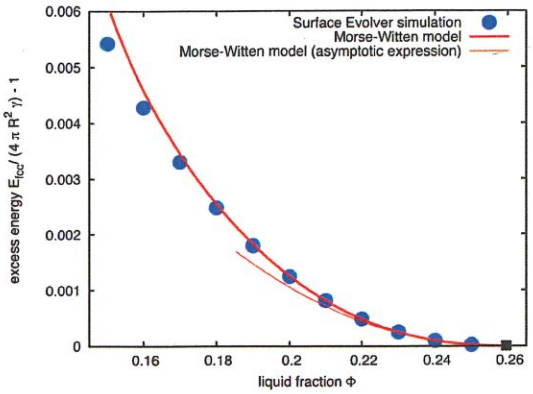

Fig. 7 Normalized excess energy $\varepsilon(\phi)$ (eqn (4)) as a function of liquid fraction for an fcc foam in the wet regime. The thick solid line is obtained from a parametric plot of the parameter-free Morse–Witten model; data points are from numerical calculations using the Surface Evolver. The thin solid line is the asymptotic form, eqn (10), obtained from the Morse–Witten model. The wet limit is marked by a black square. Note by comparison with Fig. 5 that on this energy scale the tiny difference between the excess energies of fcc and hcp would not be perceptible.

where we have expressed displacement x in terms of liquid fraction ϕ, using eqn (6). Fig. 7 shows that this asymptotic form for the excess energy (shown as thin line) provides a good approximation for values of liquid fraction exceeding about 0.22, consistent with the assertion that Morse–Witten theory is asymptotically exact in that limit.

An even better agreement of Morse–Witten theory with the Surface Evolver data for $\varepsilon_{fcc}(\phi)$ is achieved by using the parametric expressions for $\phi(x(f))$ (eqn (6) and (7)) and $\varepsilon_{fcc}(f)$ (eqn (9)). This results in a relative error less than 10% even at $\phi \simeq 0.15$, roughly half way between the dry and wet limits; see thick line in Fig. 7. Note that on the energy scale displayed in Fig. 7 it would not possible to distinguish the energies of fcc and hcp; the energy scale used in Fig. 5 is 100 times smaller.

We note in passing that the asymptotic form for the excess energy, eqn (10), is also obtained from the Z-cone model[31,32] for $Z = 12$, corresponding to the 12 contacts of an fcc bubble. In the cone model a bubble with Z neighbours is decomposed into Z identical pieces, which are approximated as circular cones. The cap of each cone consists of a flat disk (the area of contact with a neighbouring bubble) and an outer part with constant mean curvature, joining the flat disk smoothly. Within the cone model approximation, analytic expressions of surface energy as a function of liquid fraction can be derived.

5.1.2 Energy difference of fcc and hcp structure in the wet regime. All of the contacts in the two structures have displacements x_i which are the same, for any given liquid fraction ϕ. However, in the Morse–Witten theory the forces f_i and energies are not the same.

A direct approach to the evaluation of this difference is cumbersome, requiring the computation of the inverse of the displacement-force relation mentioned above and involving the Lambert function, *etc.* We have accomplished this, but in the course of exploring the problem we encountered a simpler procedure which gives essentially identical results. This consists of the evaluation of the energy difference for constant forces f_i. That is, we attribute to the hcp structure the same forces f_i as in the fcc structure with the same displacements x_i. This gives the negative of the required result, to within a very good approximation (see Appendix A).

The expression for the energy difference that this gives is

$$\varepsilon_{fcc}(f) - \varepsilon_{hcp}(f) = \frac{f^2}{8\pi}\sum_{i,j\neq i}^{12}\left(G\left(\theta_{ij}^{fcc}\right) - G\left(\theta_{ij}^{hcp}\right)\right). \qquad (11)$$

Only 9 elements of the (symmetric) 12 × 12 matrix of θ_{ij} contribute to the energy difference. These are the elements related to the angles between contacts in the AC and AA layers below and above the central bubble, as indicated in Fig. 6. The sum in eqn (11) is thus given by $6G\left(\arccos\left(-\frac{1}{2}\right)\right) + 3G(\arccos(-1)) - 6G\left(\arccos\left(-\frac{5}{6}\right)\right) - 3G\left(\arccos\left(-\frac{1}{3}\right)\right)$, leading to a remarkably simple result for the energy difference,

$$\varepsilon_{fcc}(f) - \varepsilon_{hcp}(f) = \frac{1}{16\pi^2}(-5\ln 11 + 9\ln 3 + 3\ln 2)f^2. \qquad (12)$$

The evaluation of the energy difference $\Delta\varepsilon(\phi) = (E_{fcc}(\phi) - E_{hcp}(\phi))/E_0$, between fcc and hcp (as well as the direct calculation, as mentioned above) is then obtained by combining $\Delta\varepsilon(x)$ with the parametric expressions for the displacement–force, $x(f)$, and liquid fraction $\phi(x(f))$ relationships (eqn (7) and (6), respectively). The result is shown as a thick solid line in Fig. 8, it is in excellent agreement with the direct evaluation mentioned above; moreover it supplies an analytic form in terms of liquid fraction, given below. Agreement with the Surface Evolver calculations is good, as Fig. 8 shows.

An asymptotic expression for the energy difference $\Delta\varepsilon(\phi)$ is obtained from eqn (12) using the asymptotic form for $f(x)$ (eqn (8)), together with eqn (6),

$$\Delta\varepsilon(\phi) \sim (5\ln 11 - 9\ln 3 - 3\ln 2)\left[\frac{x(\phi)}{\ln[-x(\phi)]}\right]^2, \qquad (13)$$

with displacement $x(\phi)$ given by eqn (6). This again provides a good estimate of the energy difference for ϕ exceeding about 0.24, as shown by the thin line in Fig. 8.

Having identified the source of the variation of energy in the wet limit, we will now turn to the dry limit, where an entirely different approach is required to identify the sources of the small energy differences between fcc and hcp.

5.2 Dry limit

5.2.1 Energy expansions. In the vicinity of the dry limit, where the bubble shapes are approximately polyhedral, successive contributions to the energy have been identified in the past as associated with elements of the structure (faces, borders and junctions or nodes). Fig. 9 illustrates the structural elements using two-dimensional sketches. The contribution of Plateau borders of finite width, and the further correction due to their

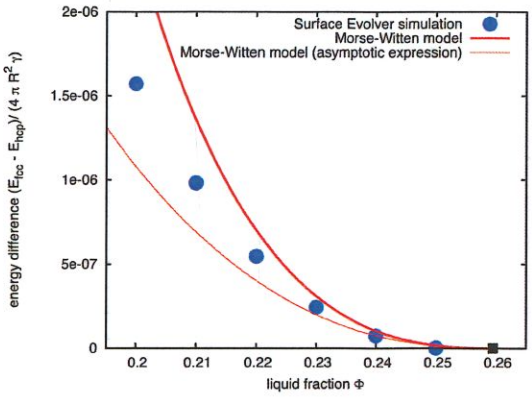

Fig. 8 Normalized energy difference $\Delta\varepsilon(\phi) = (E_{fcc}(\phi) - E_{hcp}(\phi))/(4\pi\gamma R^2)$ between fcc and hcp foams as a function of liquid fraction ϕ in the wet regime. The blue data points are computed using the Surface Evolver Software while the thick red solid line is an analytic expression resulting from the Morse–Witten model (*i.e.* a combination of eqn (6), (7) and (12)). The thin red line is the asymptotic form, given in eqn (13). The black square marks the wet limit where the energy difference vanishes.

swollen nodes (Fig. 1 and 10)[33–35] lead to an expression of energy per bubble as a function of liquid fraction ϕ of the form

$$E(\phi)/E_0 = E_{dry} - E_1\phi^{1/2} + E_2\phi, \qquad (14)$$

where E_{dry}, E_1 and E_2 are numerical constants (given in S2.3 and S2.1 for different foam structures, ESI†) and E_0 is the surface energy of a sphere with radius R (see eqn (1)). We have already noted that the first term, which survives in the dry limit ($\phi = 0$), makes no contribution to our problem. Nor does the second, as can be seen by examining Fig. 4. That is, the total line length is the same for our two structures.

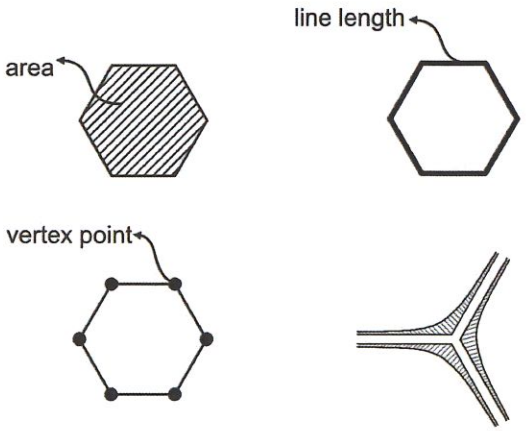

Fig. 9 Origins of the various contributions to the energy of a foam in the dry limit, as expressed by eqn (14). E_{dry} corresponds to the total film area. This is reduced by $E_1\phi^{1/2}$ due to the presence of Plateau borders of finite width, here represented as thickened lines. The presence of a vertex at their intersection leads to a further energy correction which varies linearly with ϕ in the case of a single vertex. The energy difference between fcc and hcp requires the consideration of an additional correction, see Fig. 11 and eqn (23).

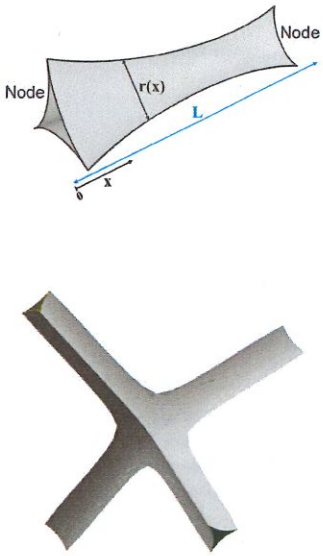

Fig. 10 Surface Evolver simulations showing part of a single Plateau border connecting two nodes and a fourfold node in a relatively dry foam (in the Kelvin structure). The cross-sectional area of the Plateau border is a function of longitudinal position x; it increases as a node is approached. Away from the node the Plateau border radius $r(x)$ is given by eqn (15) and (18).

We come next to the node term. In the present case there are two kinds of nodes, namely fourfold and eightfold, as indicated in Fig. 2. The numerical constant E_2 of eqn (14) was first calculated by,[35] applying the Surface Evolver to a single fourfold node with attached Plateau borders of finite length and taking this length to infinity by extrapolation. A more accurate value was determined by Koehler *et al.*[36] Again, a contribution from nodes which uses such an isolated constant fails to account for the energy difference in question: fcc and hcp have the same number of vertices, of the same types.

One might expect that the above expression, eqn (14), can be further extended into a series in $\phi^{1/2}$, with the next and possibly crucial term coming in as proportional to $\phi^{3/2}$, but this is illusory. Instead a subtle non-analytic form for the next correction is required. It represents the effect of the finiteness of the length of individual Plateau borders: in a sense the nodes *interact* with each other for finite ϕ; see the sketch in Fig. 11. Those interactions depend on the separations of the nodes, *i.e.* the Plateau border lengths which are different in the two structures, so at last a source of energy difference emerges. We proceed to estimate it.

Close to the dry limit, each Plateau border has a relatively small and smoothly varying cross-section as in Fig. 10, except where it merges with a node. We may describe it as having the same concave triangular cross-section as that of a uniform border, but with varying area, or radius of each of its three circular arcs. That is, the cross-sectional area $A(x) = c_g r^2(x)$ is a function of position x, along the Plateau border, where $r(x)$ is the local Plateau border radius and $c_g = \sqrt{3} - \pi/2$ is a geometrical constant.[1] In the following we write

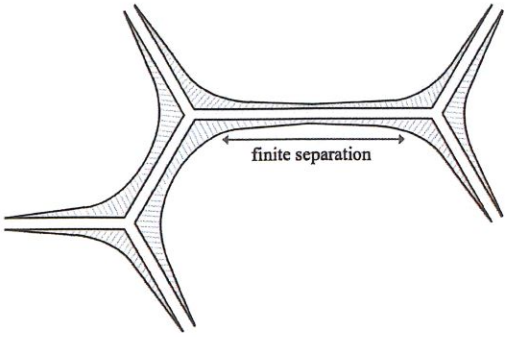

Fig. 11 Our analysis shows that the energy difference between fcc and hcp is due the different separations of their Plateau border nodes, since their contributions to the total energy are not quite independent. This results in an additional exponential term in the energy expansion of eqn (14), shown in eqn (23).

$$r(x) = r_0(1 + \delta(x)). \tag{15}$$

We will determine the appropriate form for $\delta(x)$, treated as small. Close to the dry limit this will be a good approximation along most of the length of the border, but it necessarily fails at the ends where borders are merged into a node. This point will require careful consideration in due course; see also the comments in S1 (ESI†).

For small $\delta(x)$ the Laplace–Young equation (equating local curvature with the constant pressure difference across the surface of the Plateau border) takes form of the linear differential equation

$$\frac{\mathrm{d}^2\delta(x)}{\mathrm{d}x^2} = (c_1 r_0)^{-2}\delta(x), \tag{16}$$

where $c_1 = \sqrt{\frac{2}{\sqrt{3}} - 1} \simeq 0.39$.

This has the elementary solution

$$\delta(x) = a\exp\left[\frac{x}{c_1 r_0}\right] + b\exp\left[-\frac{x}{c_1 r_0}\right]. \tag{17}$$

For the single isolated node described above, where x is the distance from the node, $a = 0$.

For a Plateau border connecting two nodes, both prefactors are non-zero. If the two nodes are identical, the swelling of the Plateau borders is described by a cosh function. (This situation is reminiscent of the catenoid shape of a soap film formed between two parallel wire rings.[37])

To our knowledge, this description of varying Plateau border cross-section has not been used before, so we provide a relatively simple illustrative example in S1 (ESI†). This is the case of the Kelvin (bcc) foam, in which all nodes are identical (and fourfold) and all Plateau borders are of equal length. (They are slightly curved, which we shall ignore.) Included in S1 (ESI†) are Surface Evolver calculations, for comparison with the approximation advanced here.

More generally, for a Plateau border connecting two nodes (which may be of different types), separated by a distance L, one obtains

$$\delta(x) = \alpha\exp\left[\frac{x-L}{c_1 r_0}\right] + \beta\exp\left[-\frac{x}{c_1 r_0}\right]. \tag{18}$$

We refer to these dimensionless numbers, α and β as node constants.

Much of the difficulty of applying this to the estimation of energies lies in the specification of the node constants (see also S1, ESI†). Using the functional form for the Plateau border profile, eqn (15) and (18), allows us to obtain a functional form also for the energy of a foam, as follows.

In order to relate Plateau border radius to liquid fraction ϕ we will use the lowest order expression $\phi = L_v c_g {r_0}^2$, where L_v is the (foam structure dependent) total length of the Plateau border network per volume of the foam. This approximation is valid in the vicinity of the dry limit, when the contribution of the swelling of the Plateau border to the total liquid content maybe neglected (*i.e.* $r(x) \simeq r_0$ throughout). In the following we will rewrite this as

$$\phi = \lambda c_g (r_0/L)^2, \tag{19}$$

with λ a structure-dependent dimensionless constant.

Consider first the approximation of a Plateau border as channel of length L and uniform cross-section (*i.e.* $\delta(x) = 0$), located at the intersection of three films, as illustrated in Fig. 1. This results in an area reduction per Plateau border by

$$\Delta a_L(r_0) = -\left(2\sqrt{3} - \pi\right) r_0 L, \tag{20}$$

Together with the scaling $L \propto \sqrt{\phi}$, eqn (19), we obtain the form of the first energy correction term in eqn (14), and no contribution to the fcc-hcp energy difference.

This overestimates the energy reduction since such straight channels overlap at the nodes. A (positive) correction to this is obtained by estimating the surface area contribution $\Delta n_{L,\alpha,\beta}(r_0)$ of the two nodes (with node constants α and β) associated with each channel of length L as

$$\Delta n_{L,\alpha,\beta}(r_0) = \left(2\sqrt{3} - \pi\right) r_0 \int_0^L \delta(x)\mathrm{d}x, \tag{21}$$

Inserting for $\delta(x)$ (eqn (18)) and integrating results in

$$\Delta n_{L,\alpha,\beta}(r_0) = \left(2\sqrt{3} - \pi\right) c_1 {r_0}^2 (\alpha + \beta)\left(1 - \exp\left[-\frac{L}{c_1 r_0}\right]\right). \tag{22}$$

Note that in the limit of $L \to \infty$ this node correction is proportional to liquid fraction ϕ; it provides the second correction term in the energy expansion of eqn (14). The finite Plateau border length adds to this an additional exponential term.

For a foam structure such as fcc or Kelvin, where all Plateau borders have the same length, one then obtains the following expression for the energy per bubble,

$$E(\phi)/E_0 = E_{\mathrm{dry}} - E_1\phi^{1/2} + E_2\phi\left(1 - \exp\left[-E_3/\sqrt{\phi}\right]\right). \tag{23}$$

The numerical constants E_1, E_2 and E_3 all depend on the type of foam structure. In S2 (ESI†) we show that E_1 and E_3 are

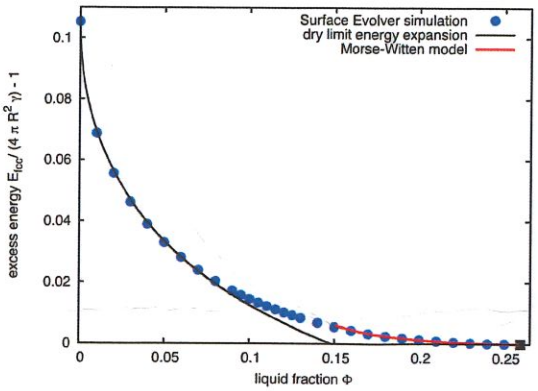

Fig. 12 Excess energy $E(\phi)/(4\pi R^2\gamma) - 1$ of an fcc bubble as a function of liquid fraction ϕ. The black line is a one-parameter fit to the dry limit energy expansion, eqn (23), resulting in $\alpha + \beta \simeq 1.3$. The red line is the energy expression from the Morse–Witten model, shown also in Fig. 7. (On this energy scale the tiny difference between the excess energies of fcc and hcp would not be perceptible, *cf.* Fig. 5.).

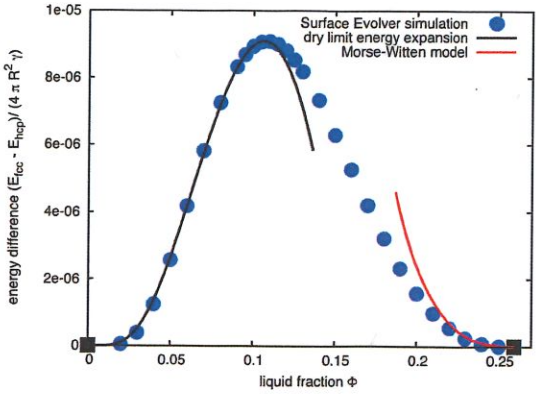

Fig. 13 Analytical estimates of the energy difference between fcc and hcp. The blue line is the dry limit energy expansion of eqn (24), for $\alpha \simeq 0.82$ and $\beta \simeq 0.2$. Other combinations are possible but describe the data over a more limited range in liquid fraction. The red line is the result from the Morse–Witten model, as shown also in Fig. 8.

readily estimated from geometry, only E_2 also involves the *a priori* unknown node constants α and β, which need to be determined from least-square fits to either energy as a function of liquid fraction, or Plateau border profiles. Fig. 12 demonstrates the validity of this energy expansion, eqn (23), for an fcc foam. (See Fig. S2, ESI†) ~~in S2~~ for its application to a (Kelvin foam.)

We will in the following show that it is the presence of the exponential terms in the energy expansion, eqn (23), resulting from finite Plateau border lengths, which can account for the energy difference between fcc and hcp.

5.2.2 Energy difference between fcc and hcp in the dry limit. We will now apply the above theory to our principal goal – the estimation of the energy difference between fcc and hcp, particularly in the dry regime. As noted above, only the corrections due to the nodes, given by $\Delta n_{L,\alpha,\beta}(r_0)$ per Plateau border of length L (eqn (22)), need to be considered for this.

The detailed calculation is presented in S2.2 (ESI†). It takes account that of the 24 edges in the hcp structure, 18 are identical to those in fcc, while 3 edges have an α node at each end and length $\frac{4}{3}L$, and the remaining 3 edges have a β node at each end and length $\frac{2}{3}L$.

This results in the following functional form for the energy difference between fcc and hcp as a function of liquid fraction ϕ,

$$\left(E_{\mathrm{fcc}}(\phi) - E_{\mathrm{hcp}}(\phi)\right)/E_0 = E_4\phi\exp\left[-E_3\Big/\sqrt{\phi}\right] \times\left\{\alpha\left(\exp\left[-E_3\Big/\left(3\sqrt{\phi}\right)\right]-1\right)+\beta\left(\exp\left[+E_3\Big/\left(3\sqrt{\phi}\right)\right]-1\right)\right\}, \quad (24)$$

as detailed in S2 (ESI†). Here again we have used the lowest order expression of (eqn (19)) for relating r_0 to ϕ. The structural constants E_3 and E_4 are readily computed as $E_3 \simeq 1.646$ (see S2.1, ESI†) and $E_4 \simeq 0.059$ (see S2.2, ESI†).

Values for the two node constants α and β can then be obtained from a least squares fit of the numerical Surface Evolver data to eqn (24). Fig. 13 shows that a two-parameter fit, resulting in $\alpha \simeq 0.82$ and $\beta \simeq 0.2$, provides an excellent description of the numerical data for liquid fraction up to about 0.12. However, the values of the fit parameters are highly dependent on the range over which the data is fitted.

In Table 1 we summarize our preliminary estimates of the node constants α and β as obtained from least square fits of numerical data. More accurate data would be required to extract data also from Plateau borders in the fcc and hcp structures.

6 Conclusion

We have described two separate exercises that provide asymptotic estimates of energy in the respective limits of dry and wet foams, directly applicable to the very small energy differences under study, with satisfactory results. Together, they give a good account of the magnitude of the very small energy difference between fcc and hcp. There is room for improvement in various details, but the analytic forms that have been identified are convincing, when compared with the Surface Evolver calculations.

Both theories depend on the particular features of this problem: no easy generalisation to other structures presents itself. That is, we do not claim to be able to formulate a general

Table 1 Summary of values for node constants α and β, together with the respective sources for their estimates

method	(α)	(β)	$(\alpha+\beta)$	$\alpha+\beta$
Kelvin, energy, Fig. S2	0.56	—	—	—
Kelvin, Plateau border profile, Fig. S1	0.9	—	—	—
Kelvin, liquid fraction, eqn (41)	0.75	—	—	—
fcc, energy, Fig. 12	—	—	1.3	—
Energy difference fcc/hcp, Fig. 8	0.82	0.2	—	1.02

theory of foam energies to higher order than eqn (23). Nevertheless the success of these analyses may provoke similar theories for small effects, where the cruder theory is inadequate.

Experiments with monodisperse bubbles of a few hundred μm in diameter have shown that these crystallize spontaneously, with a roughly 2 to 1 preference of fcc over hcp.[7,8] While this appears to be conflicting with our analytical and numerical results showing that fcc is the higher energy structure we should stress that the relative energy difference is less than 0.001% percent. The experimentally found preference for fcc may be due to dynamic hydrodynamic effects involving the mechanical stability of structures during the formation of the crystalline structure.[10]

From a theoretical perspective our results also demonstrate the usefulness of the Morse–Witten model of deformable bubbles as a promising analytical alternative to the computational modelling of crystalline foams and also emulsions, which show many analogies.[38,39] Crystalline foams have recently attracted attention as excellent candidates for self-organised photonic networks ('Phoamtonic design'), particularly the Kelvin and Weaire-Phelan structures, featuring large bandgaps.[40]

Conflicts of interest

There are no conflicts of interest to declare.

A Proof for $\Delta E_f = -\Delta E_x$

Here we will give a general derivation of the result required in 5.1.2, relating the energy difference under the condition of constant forces to that under constant displacement. It is more transparent than a more direct and detailed one.

Consider a set of forces f_i (column vector $\vec{f}$) and corresponding displacement x_i. The forces depend linearly on the displacements,

$$\vec{f} = M\vec{x},\ \vec{x} = M^{-1}\vec{f}, \tag{25}$$

where M is a matrix (not necessarily a scalar: each force depends on more than one displacement).

The energy may be written as

$$E = \frac{1}{2}\vec{x}^{\,T} M^{-1}\vec{f} \tag{26}$$

or

$$E = \frac{1}{2}\vec{f}^{\,T} M\vec{f} \tag{27}$$

Let M have the form

$$M = M_0 + M_1, \tag{28}$$

with $M_0 = \lambda I$, where I is the unit matrix and λ is a scalar. The elements of M_1 are small compared with λ.

Consider a change ΔM_1 of the matrix M_1, which represents the "non-local" coupling of all forces and displacements. Using eqn (26) and (27) the consequent change of energy of a given configuration is

$$\Delta E_f = \frac{1}{2}\vec{f}^{\,T}\Delta M\vec{f} = \frac{1}{2}\vec{f}^{\,T}\Delta M_1\vec{f} \tag{29}$$

for constant forces, or

$$\Delta E_x = \frac{1}{2}\vec{x}^{\,T}\Delta(M^{-1})\vec{f} \tag{30}$$

for constant displacement.

Here $M^{-1} = (\lambda I + M_1)^{-1} \simeq \lambda^{-1}(I - \lambda^{-1}M_1)$, so that $\Delta(M^{-1}) \simeq -\lambda^{-2}\Delta M_1$. Inserting into eqn (30) gives $\Delta E_x = -\frac{1}{2}\lambda^{-2}\vec{x}^{\,T}\Delta M_1\vec{f}$. To lowest order $x = \lambda f$, resulting in

$$\Delta E_f = -\Delta E_x, \tag{31}$$

the change in energy under the condition of constant forces or condition of constant displacement have opposite signs.

In the present case, the leading term in the Morse–Witten $x(\vec{f})$ relation, eqn (2), must first be linearised (discarding the constant), producing the term λI above, while the seond term M_1 is the matrix representation of the term involving G_{ij}. The approximations involved are very good beause the latter term is small compared to the first, in the Morse–Witten relation.

Acknowledgements

This research was supported in part by a research grant from Science Foundation Ireland (SFI) (Grant no. 13/IA/1926). A visit of AMK to the TCD Foams and Complex Systems group was funded by the TCD Visiting Professors Fund and the Dublin Graduate Physics Program. We would like to thank D. Whyte for preliminary calculations of energy differences, J. Winkelmann for extraction of Plateau border radius data, and A. Irannezhad for the preparation of various figures.

Notes and references

1 D. Weaire and S. Hutzler, *The Physics of Foams*. Clarendon Press, Oxford, 1999.
2 I. Cantat, S. Cohen-Addad, F. Elias, F. Graner, R. Höhler, O. Pitois, F. Rouyer, A. Saint-Jalmes and S. J. Cox, *Foams: structure and dynamics*, Oxford University Press, Oxford, 2013.
3 W. Drenckhan and S. Hutzler, Structure and energy of liquid foams, *Adv. Colloid Interface Sci.*, 2015, **224**, 1–16.
4 L. Bragg and J. F. Nye, A dynamical model of a crystal structure, *Proc. R. Soc. London, Ser. A*, 1947, **190**, 474–481.
5 A. M. Ganan-Calvo and J. M. Gordillo, Perfectly monodisperse microbubbling by capillary flow focusing, *Phys. Rev. Lett.*, 2001, **87**(27), 274501.
6 A. M. Ganan-Calvo, J. M. Fernandez, A. M. Oliver and M. Marquez, Coarsening of monodisperse wet microfoams, *Appl. Phys. Lett.*, 2004, **84**(24), 4989–4991.

7 A. van der Net, W. Drenckhan, D. Weaire and S. Hutzler, The crystal structure of bubbles in the wet foam limit, *Soft Matter*, 2006, **2**(2), 129–134.

8 A. van der Net, G. W. Delaney, W. Drenckhan, D. Weaire and S. Hutzler, Crystalline arrangements of microbubbles in monodisperse foams, *Colloids Surf., A*, 2007, **309**, 117–124.

9 A. van der Net, D. Weaire and S. Hutzler, Rearrangement and elimination of ordered surface layers of crystalline bubble structures due to gas diffusion, *Soft Matter*, 2009, **5**, 318–324.

10 S. Heitkam, W. Drenckhan and J. Fröhlich, Packing spheres tightly: Influence of mechanical stability on close-packed sphere structures, *Phys. Rev. Lett.*, Apr 2012, **108**, 148302.

11 A. J. Meagher, D. Whyte, J. Banhart, S. Hutzler, D. Weaire and F. García-Moreno, Slow crystallisation of a monodisperse foam stabilised against coarsening, *Soft Matter*, 2015, **11**, 4710–4716.

12 J. A. F. Plateau, *Statique Expérimentale et Théorique des Liquides soumis aux seules Forces Moléculaires*. Gauthier-Villars, Paris, 1873.

13 D. Weaire and J. P. Kermode, Computer simulation of a two-dimensional soap froth. I. Method and motivation, *Philos. Mag. B*, 1983, **48**, 245–259.

14 D. Weaire and J. P. Kermode, Computer simulation of a two-dimensional soap froth. II. Analysis of results, *Philos. Mag. B*, 1984, **50**, 379–395.

15 J. F. Nye and F. C. Frank. Hydrology of the intergranular veins in a temperate glacier, *Symposium on the Hydrology of Glaciers*, 1973, vol. 95, pp. 157–161.

16 K. A. Brakke, The Surface Evolver, *Exper. Math.*, 1992, **1**, 141–165.

17 A. M. Kraynik, D. A. Reinelt and F. van Swol, Structure of random foam, *Phys. Rev. Lett.*, 2004, **93**, 208301.

18 K. Brakke, Instability of the wet cube cone soap film, *Colloids Surf., A*, 2005, **263**(1), 4–10.

19 D. Weaire and R. Phelan, Vertex instabilities in foams and emulsions, *J. Phys.: Condens. Matter*, 1996, **8**(3), L37–L43.

20 D. G. T. Barrett, S. Kelly, E. J. Daly, M. J. Dolan, W. Drenckhan, D. Weaire and S. Hutzler, Taking Plateau into microgravity: the formation of an eightfold vertex in a system of soap films, *Microgravity Sci. Technol.*, 2008, **20**(1), 17–22.

21 Lord (Thompson, W.) Kelvin. On the division of space with minimum partitional area. *Phil. Mag.*, 24:503–514, 1887.

22 *The Kelvin problem*, ed. D. Weaire, Taylor and Francis, London, 1997.

23 D. Weaire and R. Phelan, A Counter-example to Kelvin's Conjecture on Minimal-Surfaces, *Philos. Mag. Lett.*, 1994, **69**(2), 107–110.

24 R. Gabbrielli, A. J. Meagher, D. Weaire, K. A. Brakke and S. Hutzler, An experimental realization of the Weaire-Phelan structure in monodisperse liquid foam, *Philos. Mag. Lett.*, 2012, **92**(1), 1–6.

25 D. Whyte, D. Weaire, W. Drenckhan and S. Hutzler, The relative energy of fcc and hcp foams, *Philos. Mag. Lett.*, 2015, **95**, 319–323.

26 D. C. Morse and T. A. Witten, Droplet elasticity in weakly compressed emulsions, *EPL*, 1993, **22**(7), 549–555.

27 R. Höhler and D. Weaire, Can liquid foams and emulsions be modeled as packings of soft elastic particles?, *Adv. Colloid Interface Sci.*, 2019, **263**, 19–37.

28 G. Ginot, R. Höhler, S. Mariot, A. Kraynik and W. Drenckhan, Juggling bubbles in square capillaries: an experimental proof of non-pairwise bubble interactions, *Soft Matter*, 2019, **15**, 4570–4582.

29 S. Hutzler and W. Drenckhan, *The Structure of Liquid Foams. Foam Film and Foams: Fundamentals and Applications*, CRC Press, Taylor & Francis Group, 2018, ch. 16, pp. 295–308.

30 R. Höhler and S. Cohen-Addad, Many-body interactions in soft jammed materials, *Soft Matter*, 2017, **13**, 1371–1383.

31 S. Hutzler, R. P. Murtagh, D. Whyte, S. T. Tobin and D. Weaire, *Z*-cone model for the energy of an ordered foam, *Soft Matter*, 2014, **10**(36), 7103–7108.

32 D. Whyte, R. Murtagh, D. Weaire and S. Hutzler, Applications and extensions of the z-cone model for the energy of a foam, *Colloids Surf., A*, 2015, **473**, 115–122.

33 H. M. Princen, Osmotic pressure of foams and highly concentrated emulsions. I. Theoretical considerations, *Langmuir*, 1986, **2**(4), 519–524.

34 D. Weaire, Structural transformations in foam, *Philos. Mag. Lett.*, 1994, **69**(2), 99–105.

35 R. Phelan, D. Weaire, E. A. J. F. Peters and G. Verbist, The conductivity of a foam, *J. Phys.: Condens. Matter*, 1996, **8**(34), L475.

36 S. A. Koehler, S. Hilgenfeldt and H. A. Stone, A generalized view of foam drainage: Experiment and theory, *Langmuir*, 2000, **16**, 6327–6341.

37 D. Lovett, *Demonstrating Science with Soap Films*, IOP Publishing, Bristol, Philadelphia, 1994.

38 S. Hutzler, N. Peron, D. Weaire and W. Drenckhan, The Foam/Emulsion Analogy in Structure and Drainage, *Eur. Phys. J. E: Soft Matter Biol. Phys.*, 2004, **14**, 381–386.

39 D. Langevin and W. Drenckhan, Monodisperse foams in one to three dimensions, *Curr. Opin. Colloid Interface Sci.*, 2010, **15**, 341–358.

40 M. A. Klatt, P. J. Steinhardt and S. Torquato, Phoamtonic designs yield sizeable 3d photonic band gaps, *Proc. Natl. Acad. Sci. U. S. A.*, 2019, **116**(47), 23480–23486.